2008 IEEE International Conference on
Robotics and Automation
Pasadena, CA, USA, May 19-23, 2008

3D Obstacle Detection and Avoidance in Vegetated Off-road Terrain

H. Schäfer, A. Hach, M. Proetzsch and K. Berns

Abstract— **This paper presents a laser-based obstacle detection facility for off-road robotics in vegetated terrain. In the context of this work the mobile off-road platform RAVON was equipped with a 3D laser scanner and accompanying evaluation routines working on individual vertical scans. Identified terrain characteristics are used to build up a local representation of the environment. Introducing the abstraction concept of virtual sensors the transparent integration of additional terrain information on the basis of standardized behavior modules can be achieved.**

I. INTRODUCTION

Environment perception is a crucial point in autonomous navigation and is subject to constant scientific research. Navigation through vegetated off-road terrain in particular requires elaborate obstacle detection facilities relying on special sensor systems which tend to have a rather limited field of vision. In [1] the authors proposed a biologically inspired approach to cover blind angles of sensor systems by introducing short term memories. Especially during maneuvering in narrow driving situations such local representations provide valuable information.

In this paper an obstacle detection facility for vegetated off-road terrain based on 3D laser data shall be presented. Furthermore a generic approach for covering blind angles through the concept of virtual sensors is proposed. This method is compatible with the behavior-based fusion mechanism for extending control software systems in a transparent fashion as introduced in [2]. The laser-based obstacle detection system subject to this paper was implemented and evaluated on the mobile off-road platform RAVON[1] developed in the Robotics Research Lab at the University of Kaiserslautern.

II. STATE OF THE ART

Obstacle detection is an important problem to be solved when building autonomous vehicles. In this domain a lot of success was already achieved for man-made [3] and dessert-like [5], [6] outdoor scenarios whereas intensely vegetated off-road terrain still holds many difficulties in stock. In rough terrain obstacles are no longer distinct entities which reside above or back into the ground. Obstacles rather tend to integrate into the environment such that they are difficult to discover. A rugged piece of terrain may still be passable at low speeds yet a single stone may be a threat to the robot on a severe slope. Furthermore vegetation may obstruct passages or cover hindrances such that a binary decision for traversability will no longer suffice for autonomous navigation.

Due to the precise nature of measurement laser range finders deliver valuable data for load-bearing surface analysis and vegetation discrimination. Comparing the types of analyzing 3D scans in outdoor environments, two different approaches can mainly be found. Scans are either evaluated independently [7], [8] or accumulated to a point cloud before being processed [9], [10], [4]. Processing point clouds is usually computationally very expensive and tends to require a stop-and-go mode of operation due to the registration problem[2]. Traditionally such approaches rather come from the research area of SLAM where precise metric data is required. For obstacle detection the aggregation of local terrain information suffices. Therefore an on-the-move evaluation of independent scans similar to [8] was adopted with several extensions for coping with vegetated off-road terrain.

In [11] vegetation is explicitly considered as obstructing the load-bearing surface. On the basis of 3D point clouds the ground level is estimated and when the robot passes the scanned area the actual load-bearing surface is detected using vehicle terrain interaction. That way the robot shall learn to make better estimates in the future. Coming from the field robotics area this approach does not assume that hindrances may be hidden in high grass yet the idea of load-bearing surface extraction as a first step in obstacle detection was adopted in the approach presented here.

Note that the approaches mentioned above can be sorted into two groups. Either a complete map of the environment is built up or only the most current measurements are taken into account. The former in particular in difficult terrain needs a lot of memory or has to be abstracted such that valuable information is lost. The latter makes maneuvers in narrow driving situations very complicated as no information about regions currently not covered by the sensor systems is available.

III. THE MOBILE OFF-ROAD PLATFORM RAVON

The off-road platform RAVON features a variety of sensor systems for obstacle detection [12]. Two horizontally mounted planar laser range finders (front and rear) monitor close range safety zones. A stereo camera system and a 3D laser scanner at the front side of the robot provide terrain information up to a distance of 15 m. Furthermore a spring-mounted bumper system is used to detect hindrances on a tactile basis. That way the robot may discover shortcuts

Robotics Research Lab, University of Kaiserslautern,
P.O. Box 3049, D-67653 Kaiserslautern, Germany
b_schaef@informatik.uni-kl.de

[1]RAVON → Robust Autonomous Vehicle for Off-road Navigation

[2]Registration Problem → Problem of integrating data over time with precise pose information.

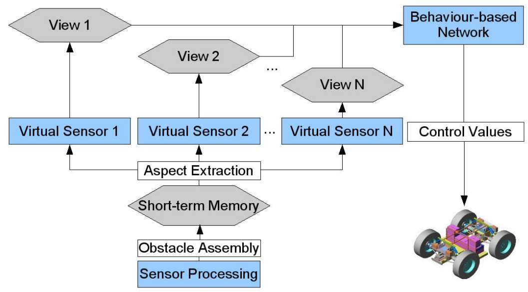

Fig. 1. Top-level concept of the obstacle detection facility.

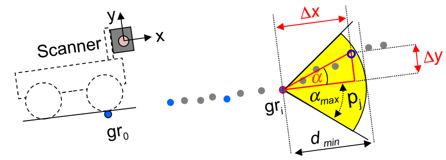

Fig. 2. Load-bearing surface analysis.

in high vegetation which cannot be detected with visual sensors alone. If structures ahead have been classified as dense yet flexible vegetation the robot drops to creep velocity (about $5\frac{cm}{s}$). The deflection of the spring-mount is constantly monitored as an indicator for rigid structures hidden in the vegetation. In such cases the robot backs off and tries to find another path. For cases of emergency the tactile facility is equipped with an industrial safety system which directly stops the robot.

The robot's 4WD with four separate motors and independent front and rear steering allow for advanced driving maneuvers like small radii or parallel steering. RAVON has the dimensions of a city car, weighs about 650 kg and can ascend and descend slopes of 45° at a max. velocity of 2 m/s.

IV. 3D-LASER-BASED OBSTACLE DETECTION

The 3D scanner on RAVON is built up using a planar *Sick lms291* (180°, angular resolution: 0.5°) mounted on a panning mechanism (active pan angle: +/- 65°, update rate: 1 Hz) such that the scanning plane is perpendicular to the ground. Every scan yields a vertical section of the terrain (see Fig. 2) which allows for a meaningful interpretation on the basis of the immanent ground references. Fig. 1 depicts the conceptual basis of the 3D laser obstacle detection facility. At first individual scans are analyzed as to ground and obstacle structures in step *Sensor Processing*. After that abstract terrain information is aggregated into the *Short-term Memory* which is then cast into independent *Views* by generic *Virtual Sensors*. Note that *Virtual Sensors* can monitor different aspects and cover arbitrary sections of the terrain separating distinct concerns. That way a generic interface for the robot's behavior-based control system is provided.

V. ANALYSIS OF INDIVIDUAL SCANS

Vertical sections of the terrain usually consist of ground and obstacle structures. First of all the load-bearing surface is estimated taking into account the vehicle's climbing capability. This results in a potentially drivable terrain contour relative to which obstacles can be judged in further processing steps.

The individual scan analysis is carried out in the scanner local coordinate frame as indicated in Fig. 2. To reflect the vehicle capabilities in an absolute context the pan angle as well as vehicle roll and pitch are applied to the scanner data. The angular resolution of the scanner limits the effective range of the adopted approach to approx. 20 m as the sample density becomes too low. Therefore, coordinates which are far away from the vehicle are discarded. Note that this is not a limitation given the max. vehicle velocity of 2 m/s. The remaining samples are sorted ascending by x-distance.

A. Load-bearing Surface Extraction

The ground may (partially) be hidden by vegetation. However, as long as the vegetation is not too dense samples originating from penetrating laser beams permit the approximation of the load-bearing surface by iterative determination of ground representatives (gr_i). As a reference the ground point gr_0 is introduced which resides beneath the front wheels as these are assumed to have ground contact. Starting from the predetermined ground representative gr_0 all following representatives are determined in relation to their respective predecessor (see Equation Set 1 and Fig. 2). Based on the current representative gr_i the points with greater x-distance within the vehicle's climbing limit $\alpha_{\max}$ are considered (M_i). The candidate set C_i is filled with points from M_i within the search distance $d_{\min}$. If no candidates is in this interval the search continues until a suitable point is found or no points remain in M_i. From the set of candidates C_i the point with the least slope and the point with the smallest y-value are identified. The point with the largest x-distance then becomes the following ground representative. That way a uniform distribution of ground representatives is achieved.

$$
\begin{aligned}
M_i &= \{p \in SP \mid gr_{ix} < p_x \wedge |\alpha(p,i)| < \alpha_{\max}\} \\
C_i &= \{p \in M_i \mid p_x \leq \max(gr_{ix} + d_{\min}, x_{\min}(M_i))\} \\
gr_{i+1} &= x_{\max}(\alpha_{\min}(C_i, i), y_{\min}(C_i)) \qquad (1)
\end{aligned}
$$

where

$$
\begin{aligned}
p &= (p_x, p_y), \quad gr_i = (gr_{ix}, gr_{iy}) \\
\alpha(p,i) &= \tan\left(\frac{gr_{iy} - p_y}{gr_{ix} - p_x}\right) \\
x_{\min}(M) &= p \text{ with } p_x \leq b_x \ \forall\, b \in M \\
\alpha_{\min}(M,i) &= p \text{ with } \alpha(p,i) \leq \alpha(b,i) \ \forall\, b \in M \qquad (2) \\
y_{\min}(M) &= p \text{ with } p_y \leq b_y \ \forall\, b \in M \\
x_{\max}(p1,p2) &= \begin{cases} p1, & \text{if } p1_x > p2_x \\ p2, & \text{else} \end{cases}
\end{aligned}
$$

Based on the distance to the lines defined through successive ground representatives the remaining points are assigned to five classes (See Fig. 3). In general *sky* points can be ignored as the robot can pass under the structure in question. Points labeled as *ground* mean no harm to the

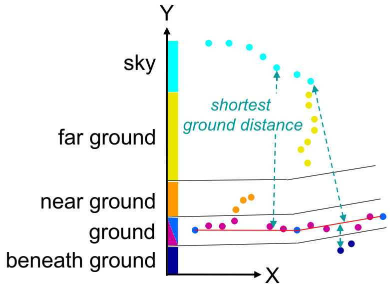

Fig. 3. Ground distance as classification criterion.

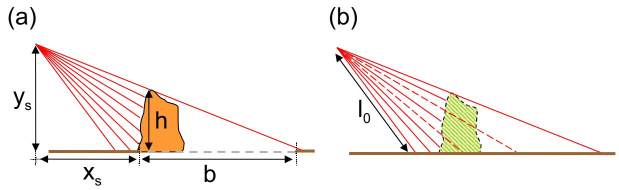

Fig. 4. Solid obstacle (a) vs. flexible vegetation (b).

vehicle either but are used to estimate the terrain roughness. Representatives labeled as *beneath ground* potentially belong to negative obstacles. Both terrain roughness and negative obstacle analysis is described in Section V-C. Members of class *near ground* represent structures which are traversable at low speeds whereas members of class *far ground* mark insurmountable entities. Both classes are subject to the further classification in the vegetation discrimination step which determines the severity of corresponding structures.

B. Vegetation Discrimination

In off-road environments vegetation is one of the key issues to be addressed in obstacle detection. Flexible vegetation covering the ground is drivable, solid obstacles in contrast are not. Therefore, it is necessary to distinguish between these entities. Vegetation as far as it is not too dense is partially penetrable by laser beams whereas solid obstacles shadow large parts of the ground (see Fig. 4). The maximum obstacle height h can be approximated employing the intercept theorem. If the shadowed ground indicates that an obstacle exceeds the capabilities of the vehicle all scan points between the two bordering ground points are marked as solid. Note that points *near ground* classified as vegetation can be traversed by the robot without harm. For points labeled as *far ground* the context of further clustering has to be taken into account as such entities may cause damage to the sensor phalanx.

C. Terrain Roughness Analysis

To estimate the roughness of the terrain regression lines are successively fit into subsets of the ground representatives which can be covered with one vehicle length each. Note that these subsets will represent overlapping sections of the terrain. For each section the variance of the *ground* points to the regression line is computed as a measure for the terrain roughness.

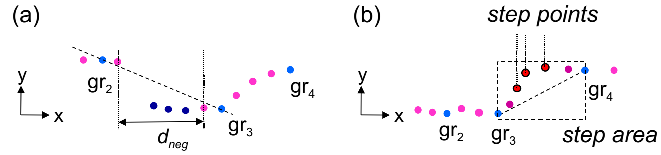

Fig. 5. Negative obstacle (a) and positive step (b).

Based on the preclassification introduced above, negative obstacles and steps can be determined as follows (see Fig. 5). Points classified as *beneath ground* represent a negative obstacle if the length d_{neg} of such a region exceeds half the wheel diameter (i.e. 40 cm for RAVON). If the slope of the flanking *ground* representatives exceeds the maximal descending capability of the robot a negative obstacle is registered, as well.

Steps are regions with positive slope including points not labeled as *ground* exceeding the robots' climbing capabilities.

D. Clustering Of Dense Regions

Subsequent to the classification, all points except *ground* points are clustered using the DBSCAN algorithm [14]. Note that the clustering radius in this implementation increases with distance to reflect the polar nature of laser scanner data. Furthermore the algorithm was extended with compatibility rules which allows for mixed clusters if the following criteria are met.

If a region of *far ground* points is both close-by *ground* and *sky* an insurmountable positive obstacle cluster is registered. If a region of *far ground* points is standalone or has contact to *sky* an overhanging obstacle was detected. Vegetation detection via the tactile facilities is forbidden as the bumper will pass under the structure in question. Even if penetration analysis indicates flexible vegetation both of these obstacle types have to be considered as critical because they might damage the 3D laser scanner or the camera systems. A region of *far ground* points exclusively close-by *ground* is surmountable in case the entity represents flexible vegetation and is no threat to the sensor phalanx. Even if such a structure is not classified as vegetation a tactile investigation is possible as the bumper is bound to hit a potentially harmful entity forcing the robot to back off.

VI. SHORT TERM MEMORY

In order to retain information about the ground contour and obstacles detected by the sensor system a representation of the vicinity of the vehicle is necessary. This information is the basis for the control system's evasive behaviors. Inspired by the multi level approach presented in [13] the short term memory for RAVON's horizontally mounted laser scanners [1] was extended such that detailed obstacle information – as provided by the analysis of the vertical scans – can be stored. For complicated ranking maneuvers in narrow driving situations a frequently updated representation of the local terrain is mandatory. In contrast global metric knowledge (i.e. a long term memory) is not necessary and

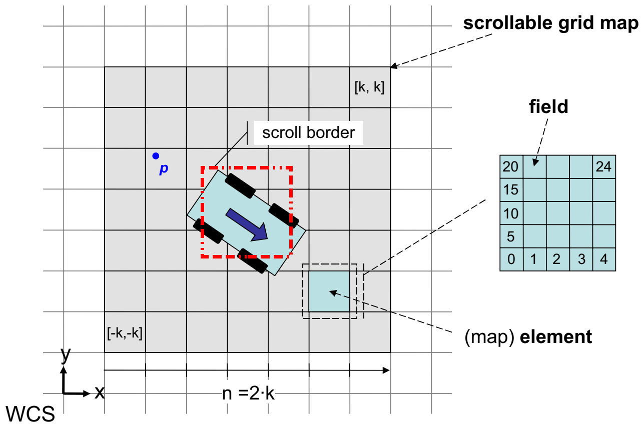

Fig. 6. Structure of the grid map.

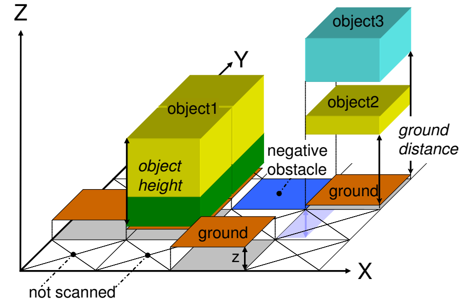

Fig. 7. Example of a filled grid element.

tends to be more difficult to handle due to update effort and error sources like localization deviation over time. For these reasons the authors propose to restrict the monitored area which furthermore avoids problems concerning the amount of required storage and computational costs for data retrieval.

A. Absolute Local Grid Map

Fig. 6 shows the structure of the grid map used for terrain representation. The orientation of the map is fixed and coaxial with the absolute working coordinate system (WCS) of the robot. Ground and obstacle structures are stored in the corresponding map *elements* on the basis of coordinates in the WCS. The map is scrolled row-wise or column-wise every time the robot crosses the scroll border such that the vehicle always resides in the center of the absolute map. Oscillation is avoided by setting the center area slightly larger than one map element. Scrolling is implemented using simple modulo arithmetic in combination with clearing the row or column in question. Each map element was chosen to have a side length of $1\,m$ to achieve a suitable scrolling granularity with respect to the robot dimensions and velocity. By dividing every element into 25 *fields* the final grid size is $20\,cm^2$ which corresponds to the contact area of one wheel.

B. Filling the Map

After the scan analysis representatives for ground and obstacle structures are determined and assigned to the map elements. In that context information of consecutive scans is be merged and older data is updated. Each of the 25 fields in one map element can either be in status *unknown* or filled with information about roughness, slope and elevation. In addition to the ground information, fields can contain obstacle information which is grouped to objects if applicable. Fields with obstacle information originating from the same cluster of one scan (see Section V-D) are always grouped. Neighboring fields of different scans are grouped if their obstacle characteristics are the same. Fields representing traversable entities are never merged with fields reflecting obstacle structures. Both aspects are stored in separate super adjacent objects as indicated in Fig. 7. At the moment object merging is limited to the scope of one map element. The objects contain the ground distance, the height over ground and classification information as well as the result of the vegetation estimation.

VII. VIRTUAL SENSORS AS INTERFACE TO THE BEHAVIOR-BASED NETWORK

On the one hand, there is the grid map keeping detailed information about the vicinity of the robot. On the other hand, there are a lot of behavior modules requiring only particular aspects of this information. Furthermore they do not monitor the whole map but only regions relative to the robot. So a second representation layer, in the following called *virtual sensors*, is used as an interface to the behavior-based network. These virtual sensors are defined relatively to the robot. Each sensor evaluates a part of the grid map and considers different aspects of the stored information. As data structure for these virtual sensors a sector map is used. The implementation of this map allows the definition of different sector types like Cartesian and polar ones, containing the shortest distance to an obstacle, a rating, and further information required by a corresponding behavior. Each region is observed by two sensors i.e. two maps per region are created. One map is for critical obstacles only, the other is for all obstacle types. This fragmentation of information permits the usage of one and the same behavior module for different aspects. The impact on the vehicle motion, which must of course be different for critical and non-critical obstacles, is then determined by the arrangement of behavior modules inside the behavior-based control network. Therefore, by using these maps the behavior modules are independent of the lower representation structures or real sensors. This provides further advantages like better integrability, traceability and testability.

VIII. EXPERIMENTAL RESULTS

A. Static Forest Scene

Fig. 8 shows RAVON at the border of a forest. The corresponding grid map – recorded while driving to this position – can be seen in Fig. 9. For better visualization the content of the map is split up into four parts. Map (a) contains all scanned ground fields (circles) and objects near ground (dots). These objects are traversable without risk. Map (b) shows obstacles having contact to the ground. If their height is no threat to the sensor systems (circles), a

Fig. 8. RAVON located at the border of a forest

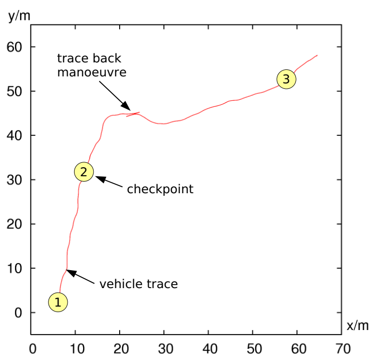

Fig. 11. Path of the autonomous driving experiment

tactile creep maneuver is allowed, even if the structures are classified as solid. Overhanging obstacles (circles) and large obstacles with contact to ground and sky like trees (dots) are plotted in (c). Map (d) shows overhanging clusters which are nonhazardous as these have ground distance above the robot height.

Based on the grid map, the sector maps shown in Fig. 10 are derived. Maps (a) and (b) contain the shortest distance to any obstacle per sector accompanied with a severity rating independent of the obstacle type. Obstacles with a rating below 0.5 (light gray) are traversable at reduced speed. Obstacles rated above 0.5 (dark gray) may be tested in a tactile maneuver. Maps (c) and (d) contain only critical obstacles which have to be evaded in any case.

B. Autonomous Driving Experiment

The process of building up the local obstacle map and the evaluation of vehicle reaction on terrain properties is the focus of the second experiment. Here the vehicle drives autonomously on a path through a forest area as shown in Fig. 11. Three checkpoints are given which are referred to in Fig. 12 showing an image of the scene and the corresponding obstacle maps. Checkpoint (1) shows the start of the experiment. The obstacle map is filled only in front of the robot showing several objects identified as critical obstacles. Additionally the terrain roughness estimation shows the edge of the path in front of the vehicle. The figures also show the affected sectors at the front indicated by gray (normal) and black (critical) lines.

At checkpoint (2) a high degree of vegetation forces the robot into the tactile creep mode making it squeeze through the tight path. A large area containing critical obstacles is perceived to the right of the robot, as well. Between checkpoint (2) and (3) vegetation causes the vehicle again to drop to creep velocity. As the bumper detects an obstacle hidden in the grass the robot backs off and through a slight correction of the path the robot manages to evade the obstacle continue its path. Finally, checkpoint (3) shows the end of the run with well distinguishable critical and non-critical areas.

IX. CONCLUSION AND FUTURE WORK

In this paper a method for obstacle detection in 3D laser data was proposed. A load-bearing surface analysis followed by the classification of points into obstacle classes – which are finally clustered – makes explicit filtering of outliers unnecessary. That way the integral nature of obstacles in vegetated off-road terrain is accounted for. Furthermore the concept of a short term memory was successfully adopted in order to cover blind angles of the sensor system. Using the concept of virtual sensors monitoring different aspects and ranges of the short term memory a generic abstraction layer was introduced which supports transparent integration into the robot's control software according to [2].

The implemented system was evaluated using the semi-autonomous tele-operation mode in the challenging *non-urban* scenario during the second *ELROB*[3]. RAVON was the only vehicle featuring autonomous obstacle avoidance in the field and acquired a respectable third place. Furthermore several kilometers of test runs were carried out fully autonomously yielding robust results in obstacle avoidance and maneuvering.

In combination with the bumper system the proposed vegetation discrimination approach is a powerful tool to detect shortcuts on a tactile basis. Yet the robot is in creep mode still very slow. In order to compensate this an additional evaluation unit for the laser data is currently under development. Rather than considering the laser sample points only a statistical voxel penetration analysis shall be used to tell flexible from solid entities.

REFERENCES

[1] H. Schäfer and M. Proetzsch, K. Berns. Obstacle Detection in Mobile Outdoor Robots - A Short-term Memory for the Mobile Outdoor Platform RAVON *International Conference on Informatics in Control, Automation and Robotics (ICINCO)*, Angers, France 2007

[2] H. Schäfer, M. Proetzsch, K. Berns. Extension Approach for the Behaviour-Based Control System of the Outdoor Robot RAVON *Autonome Mobile Systeme*, Stuttgart, Germany 2005

[3] Z. Sun, G. Bebis, R. Miller. On-road vehicle detection using optical sensors: a review *IEEE/ITSC International Conference on Intelligent Transportation Systems*, Washington, D.C.,USA 2004

[4] N. Vandapel, D. Huber, A. Kapuria, M. Hebert. Natural Terrain Classification using 3-D Ladar Data. *IEEE/ICRA International Conference on Robotics and Automation*, New Orleans, USA 2004.

[5] David Bonnafous, Simon Lacroix, Thierry Simon. Motion generation for a rover on rough terrain. *IEEE/RSJ International Conference on Intelligent Robots and Systems* 2001.

[3] ELROB → European Land Robot Trial – http://www.c-elrob.eu/

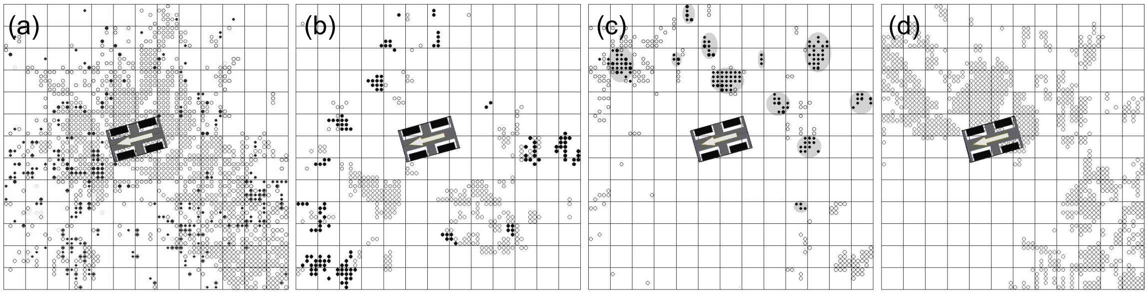

Fig. 9. Terrain characteristics contained in the grid map during the forest scenario

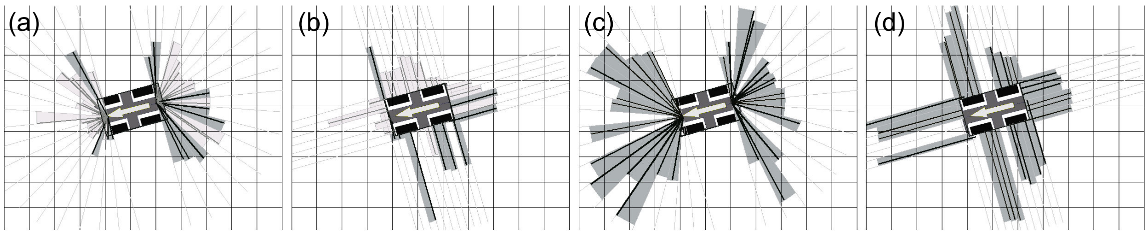

Fig. 10. Sector maps of the forest scenario: polar (a) and Cartesian (b) sector map containing shortest distance to any obstacle per sector; polar (c) and Cartesian (d) sector map containing shortest distance to critical obstacles

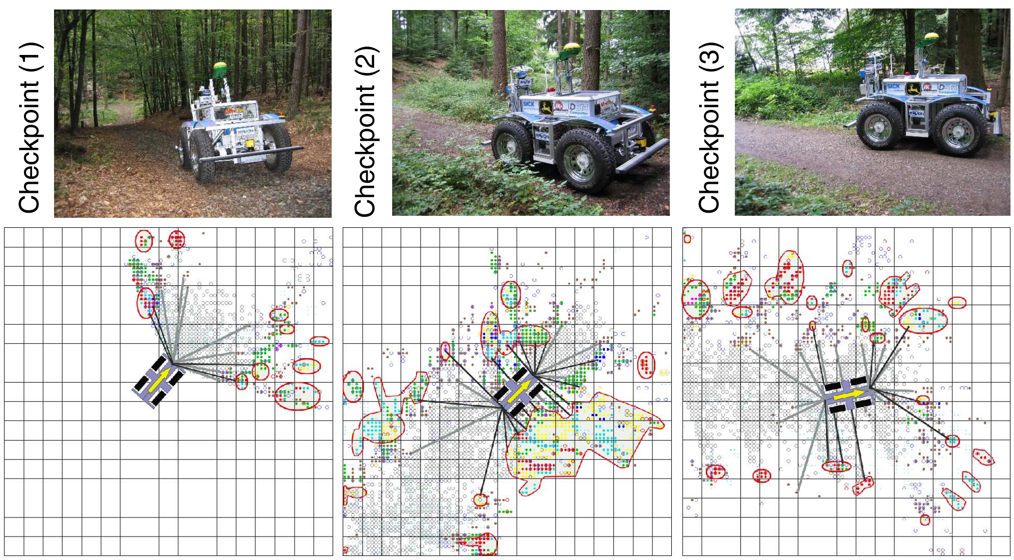

Fig. 12. Images and obstacle maps of the autonomous path scenario.

[6] K. Patel, W. Macklem, S. Thrun, M. Montemerlo. Active Sensing for High-Speed Offroad Driving. *IEEE/ICRA International Conference on Robotics and Automation*, Barcelona, Spain 2005.

[7] T. Hong, M. Abrams, T. Chang, M. Shneier. An Intelligent World Model for Autonomous Off-Road Driving. *Computer Vision and Image Understanding* 2000.

[8] P. Batavia, S. Singh. Obstacle Detection in Smooth High Curvature Terrain. *IEEE/ICRA International Conference on Robotics and Automation*, Washington D.C., USA 2002.

[9] A. Nüchter, K. Lingemann, J. Hertzberg. Extracting Drivable Surfaces in Outdoor 6D SLAM. *Proceedings of the 37rd International Symposium on Robotics (ISR)* 2006.

[10] C. Brenneke, O. Wulf, B. Wagner. Using 3D Laser Range Data for SLAM in Outdoor Environments. *IEEE/IROS International Conference on Intelligent Robots and Systems*, Las. Vegas, USA 2003.

[11] C. Wellington, A. Stentz. Online Adaptive Rough-Terrain Navigation in Vegetation. *IEEE/ICRA International Conference on Robotics and Automation*, New Orleans, USA 2004.

[12] H. Schäfer, K. Berns. RAVON - An autonomous Vehicle for Risky Intervention and Surveillance. *IARP/RISE Workshop*, Bruxelles, Belgium 2006

[13] R. Triebel, P. Pfaff, W. Burgard. Multi Level Surface Maps for Outdoor Terrain Mapping and Loop Closing. *IEEE/IROS International Conference on Intelligent Robots and Systems*, Beijing, China 2006.

[14] M. Ester, H. Kriegel, J. Sander, X. Xu. A Density-Based Algorithm for Discovering Clusters in Large Spatial Databases with Noise. *International Conference on Knowledge Discovery and Data Mining*, Portland, USA 1996.

ACKNOWLEDGMENTS

Team RAVON thanks the following companies for their technical and financial support: IK elektronik, Mayser Safety Systems, Hankook Tyres, MiniTec, SICK, DSM Computer, Hübner Giessen, and John Deere.